ACS SyntheticBiology

pubs.acs.org/synthbio

Research Article

Establishment of a Biosensor-based High-Throughput Screening Platform for Tryptophan Overproduction

Yongfei Liu, Huiling Yuan, Dongqin Ding, Huina Dong, Qinhong Wang, and Dawei Zhang*

Cite This: *ACS Synth. Biol.* 2021, 10, 1373–1383

Read Online

ACCESS | Metrics & More | Article Recommendations | Supporting Information

ABSTRACT: With the flexibility to fold into complex structures, RNA is well-suited to act as a cellular sensor to recognize environmental fluctuations and respond to changes by regulating the corresponding genes. In this study, we established a high-throughput screening platform to screen tryptophan high-producing strains from a large repertoire of candidate strains. This platform consists of a tryptophan-specific aptamer-based biosensor and fluorescence-activated droplet sorting technology. One mutant strain, with a 165.9% increase in Trp titer compared with the parental strain, was successfully screened from a random mutagenesis library. Sequencing results revealed that a total of 10 single-nucleotide polymorphisms were discovered in the genome of the mutant strain, among which CRP(T29K) was proven to significantly increase Trp production through improving the strain's tolerance of the harsh environment during the stationary phase of the fermentation process. Our results indicate that this strategy has great potential for improving the production of other amino acids in *Escherichia coli*.

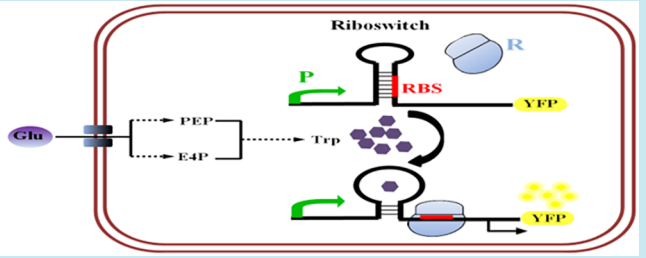

KEYWORDS: *biosensor, fluorescently activated droplet sorting (FADS), tryptophan, CRP*

One of the biggest advantages of synthetic biology is the ability to synthesize compounds that previously could not be synthesized by natural microorganisms through cascading enzymes from various species in a recombinant host strain. So far, synthetic biology has been successfully applied to synthesize a plethora of value-added compounds that are extensively used in the food, cosmetic, pharmaceutical, and healthcare industries.[1,2] Although huge efforts have already been directed toward bioprocess optimization, the production efficiency of the target compounds still cannot satisfy the industrial demand, which is mainly due to the lack of a clear understanding of the physiological and genetic background of host microorganisms. Therefore, the effects of targeted strain modifications typically result in unwanted consequences because the complex interconnected network of reactions is always strictly controlled by different layers of metabolic regulations. As a complement, many researchers have adopted semirational design strategies to improve a strain's performance. Specifically, a large mutant library with diverse phenotypes is constructed via random mutation, and the desired phenotypes are successfully selected through high-throughput screening (HTS) techniques.[3] However, this strategy is only available to select excellent variants with specific phenotypes, and it is still a daunting task to screen variants that produce inconspicuous compounds.

Genetically encoded biosensors are often employed as powerful tools for timely and precisely monitoring compounds without an obvious signal. An ideal biosensor can sensitively and specifically recognize the target compounds and couple intercellular signals to downstream signaling responses.[4] Riboswitch, one class of RNA sensors, can recognize intracellular small-molecule compounds with high specificity and affinity and regulate the expression of downstream metabolic genes on transcriptional, translational, or post-translational levels. A typical riboswitch is composed of an aptamer domain and an expression platform.[5−7] When a ligand compound binds to the aptamer domain, a conformational change in the aptamer domain will change the expression level of the expression platform.[7] So far, various types of natural riboswitches have been discovered and characterized. The ligand molecules range from ions[8,9] to enzymatic cofactors, such as thiamine pyrophosphate (TPP),[10] *S*-adenosylmethionine (SAM),[11] and vitamin B12 (VB_{12}).[12] In addition to the natural riboswitches, researchers have developed several strategies to construct artificial riboswitches for certain metabolites.[13,14] One method, called "*in vitro* selection or systematic evolution of ligands by exponential enrichment" (SELEX),[15] allows an iterative process to continuously select the specific-binding RNA molecules from a random aptamer library. It is, in principle, possible to develop diverse synthetic

Received: December 28, 2020
Published: June 3, 2021

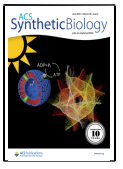

https://doi.org/10.1021/acssynbio.0c00647
ACS Synth. Biol. 2021, 10, 1373–1383

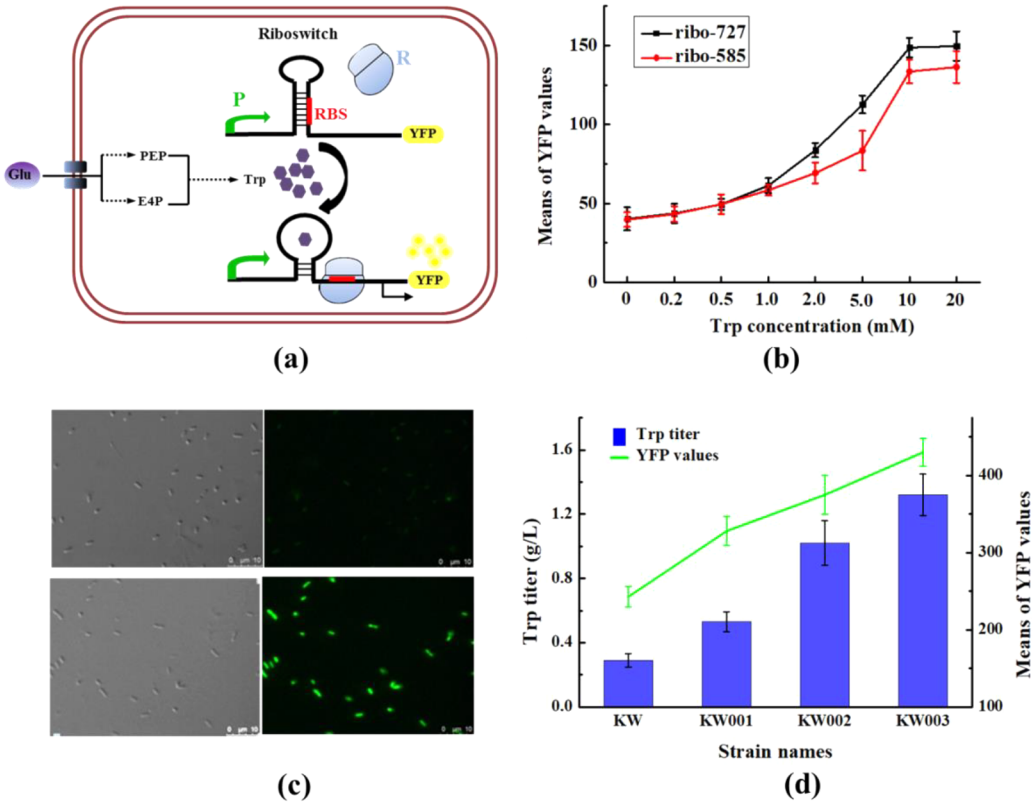

Figure 1. Design and characterization of the Trp-based biosensors. (a) Schematic diagram of the biosensor principle. When intracellular Trp is lacking, a stem-and-loop structure forms, preventing the ribosome from binding to the ribosome binding site (RBS), so the translation is terminated. When the intracellular Trp is in excess, the Trp molecule can bind the loop and change the structure, so the RBS is exposed, and translation can proceed. In the Trp biosensor, YFP can serve as a report signal so that the intracellular concentration of Trp is coupled to the YFP value. (b) YFP values of *E. coli* carrying p15-ribo585 or p15-ribo727 in response to increasing Trp concentrations in the medium. (c) Fluorescence microscopy images of *E. coli* carrying p15-ribo727 fed with (lower row) or without (upper row) the addition of Trp. (d) Fluorescence values of four defined strains carrying p15-ribo727.

riboswitches with high affinity and specificity.[16−18] In view of the above, riboswitches have been widely employed to reconstruct genetic circuits and to reprogram cellular behaviors.[18−20]

In addition to the biosensor, it is important to develop an HTS method to screen improved functional mutants from the mutation library. The microtiter-plate-based screening assay is the most commonly used screening format. The disadvantages of this screening format include: (a) Its throughput is limited to 10^3 to 10^4 cells/day, and (b) many consumables are required even though expensive colony pickers and automated liquid handling systems are equipped. Fluorescence-activated cell sorting (FACS) is a modern cell analysis technique that is extensively used to qualitatively or quantitatively detect cells' physiological properties and functional status. This technology enables researchers to analyze cells with the throughput of up to 10^7 cells/h with high accuracy.[21] In addition, droplet-based microfluidics has been recently developed as a powerful technique for single-cell screening owing to its significantly higher throughput and low assay volume.[22] Droplets of nanoliter to picoliter volumes can be generated at a speed of 10^3 droplets/s.[23] Droplets are stabilized using biocompatible surfactants to prevent coalescence and can be collected off-chip for longer incubation. Additional reagents can be injected into these droplets by using a pico-injection device. The flexibility of droplet manipulation on microfluidic devices further broadens its application in performing more complex assays.

In this article, we established an HTS platform by combining droplet microfluidic screening technology and a biosensor to select improved Trp producing strains. Mutant strains from an ARTP (atmospheric and room temperature plasma)-based whole-genome random mutation library were encapsulated in the droplet, and fluorescence-activated droplet sorting (FADS) was used to screen the encapsulated cells based on their fluorescence values. Through this platform, we identified one Trp producer with a higher Trp titer than its parental strain. The mutation sites that contributed to the improvement in the strain's performance were identified via genome sequencing, and their mechanisms were also elucidated.

RESULTS AND DISCUSSION

Design and Characterization of the Trp Biosensor. Figure 1a shows a schematic diagram of the principle of the biosensor. This biosensor consists of two sections: (1) a Trp-specific riboswitch that changes its secondary structure and activates the expression level of the downstream gene in response to elevated levels of Trp and (2) the yellow fluorescence protein (YFP) that acts as a reporter gene for the characterization of biosensors or a selecting marker for the HTS of hyperproducing strains. To demonstrate its feasibility, two synthetic Trp aptamers with different structures were employed to construct plasmids p15-ribo585 and p15-ribo727, respectively.[24] The sequences of ribo585 and ribo727 are shown in Table S2. Plasmids p15-ribo585 and p15-ribo727

https://doi.org/10.1021/acssynbio.0c00647
ACS Synth. Biol. 2021, 10, 1373−1383

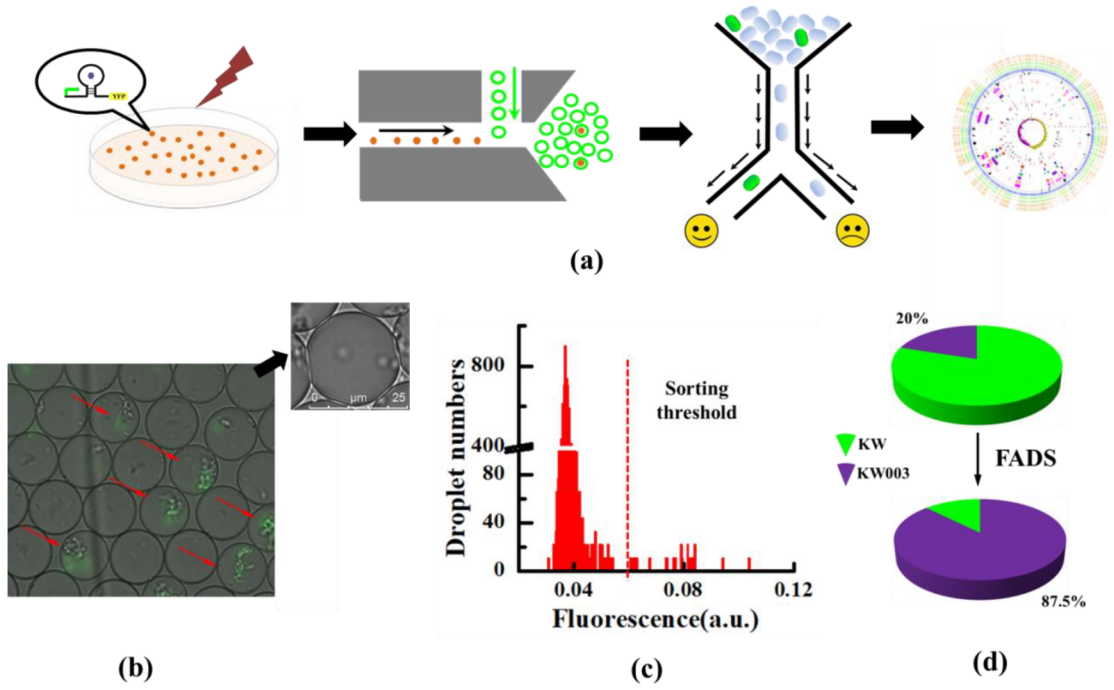

Figure 2. Establishment and characterization of the HTS platform for Trp hyperproducing strains. (a) Workflow of the HTS platform. (b) Fluorescence images of *E. coli* cells encapsulated by the droplet. The diameter of the droplet was estimated to be nearly 25 μm. The cell-to-droplet ratio was determined to be around 1:5. Droplets pointed to by red arrows represent cell encapsulation by droplets. (c) FADS results of the KW003 and KW strains mixed at a ratio of 1:4. Droplets with the top 1% of YFP values were selected for PCR analysis. (d) Percentage of KW and KW003 before FADS (upper) and after FADS (lower).

were separately transformed into the *E. coli* DH5α strain and cultivated in M9 medium fed with elevated concentrations of Trp. As shown in Figure 1b, both sensors exhibited increased YFP values in response to elevated concentrations of Trp from 0.2 to 10 mM and appeared to plateau when the additional Trp was >10 mM, indicating that the dynamic ranges of Trp for both sensors were 0.2−10 mM. Specifically, the YFP value of p15-ribo585 gently increased from 0.2 to 5 mM Trp and then significantly increased from 5 to 10 mM Trp. In contrast, the YFP values of p15-ribo727 steadily increased, accompanied by elevated Trp concentrations from 0.2 to 10 mM. The sensitivity of p15-ribo727 toward Trp was 10.85 relative fluorescence units (RFU)/mM Trp within the dynamic range, which was 1.16 times higher than that of p15-ribo585 (9.38 RFU/mM Trp). In addition, the biosensor's sensitivity toward low concentration of ligand molecule is an important factor when evaluating its performance. The sensitivity of p15-ribo727 was 1.66 times higher than that of p15-ribo585 when 0.2−5 mM of Trp was fed (14.5 *vs* 8.7 RFU/mM Trp). Overall, although p15-ribo727 presented the same dynamic range as p15-ribo585, it exhibited higher sensitivity toward Trp than p15-ribo585, especially in the low concentration of Trp. In addition, the specificity of p15-ribo727 toward other amino acids was investigated. Results showed that p15-ribo727 had little or no response toward 19 other amino acids (Figure S1), demonstrating that p15-ribo727 showed a high specificity toward Trp. Next, the fluorescence microscopy images of *E. coli* DH5α carrying p15-ribo727 fed with or without 10 mM Trp were observed. When Trp was added to the medium, a significant increase in YFP fluorescence was observed by fluorescence spectroscopy (Figure 1c). These results demonstrated that the signal of intracellular Trp level could be transformed into a visual optical readout via p15-ribo727. Furthermore, we transformed p15-ribo727 into four Trp-producing strains that exhibited increased Trp productivity. These four strains were cultivated in shake flasks in parallel and the YFP values were detected. As expected, the YFP values of four strains were positively related to their Trp titers (Figure 1d). Taken together, p15-ribo727 presented a low threshold, high sensitivity, and broad dynamic range in response to Trp. The well-behaved characteristics of p15-ribo727 suggested its agreeable practicality for subsequent HTS.

Establishment of the HTS Platform. To screen mutants with improved performance from a large mutant library, an HTS platform was constructed by combining Trp biosensor and droplet microfluidic technology. The workflow of this platform is shown in Figure 2a. Successful screening relies on the robust sorting of microfluidic droplets via their fluorescence values. First, the ratio of cell to droplet was calculated using the Poisson distribution to guarantee that the droplets were occupied by a single cell.[22] The cell-to-droplet ratio was determined to be around 1:5 (Figure 2b), which struck a balance between the throughput of FADS and avoidance of the coencapsulation events. The diameter of the droplet was ∼25 μm (Figure 2b). After encapsulated in microfluidic droplets, cells were incubated off-chip overnight to allow for cell growth and Trp production. Following incubation, the droplets were reinjected into the chip and sorted based on the fluorescence values. Droplets with the top 1% of YFP values were collected (Figure 2c) and broken by the addition of 1*H*,1*H*,2*H*,2*H*-perfluorooctanol. Then, two Trp producers, KW and KW003, were selected to investigate the platform's screening efficiency. The two strains carrying p15-ribo727 were mixed at a 1:4 ratio (KW003:KW) and sorted by the HTS platform. As expected, nearly 87.5% of sorted cells were identified as KW003 (Figure 2d). The enrichment ratio

https://doi.org/10.1021/acssynbio.0c00647
ACS Synth. Biol. 2021, 10, 1373−1383

of KW003 reached 4.4. This demonstrated that FADS efficiently enriched a small proportion of high-fluorescence droplets from a large number of low-fluorescence ones in a robust manner.

Next, we applied this platform to screen high-performance production strains from an ARTP-based genome-wide random mutation library. The optimal mutation time of KW003 was determined to be 18 s based on the criterion that the mortality was roughly 90% (Figure S2). After the mutation library was constructed, mutants were encapsulated and sorted by a droplet microfluidic platform at a throughput of 300 droplets/s. The sorted droplets were collected and seeded on agar plates. After cultivation at 37 °C overnight, a total of 192 colonies were picked up and cultivated in 96-well microtiter plates. As a control group, colonies randomly picked from the mutagenesis library were cultured under the same conditions. The Trp titers of candidate colonies were detected by a methoxydiethyl acetic acid (MAA) assay in 96-well microtiter plates. Results indicated that after screening through the HTS platform, 10.4% (20/192) of strains showed an excess 15% improvement in Trp titer, whereas 5.2% (10/192) strains showed an excess 15% decrease in Trp titer compared with parental strain KW003 (Figure 3). It is worth mentioning that the top-performing strain (K3mu1) produced 2.19 g/L Trp, an increase of 155.1% compared with KW003. The intracellular concentration of Trp of K3mu1 was 0.027 g/L (Figure S3a), which was 1.37 times higher than that of KW003 (0.019 g/L), indicating that the concentration of extracellular Trp for K3mu1 and KW003 showed a positive relationship to their intracellular Trp levels. On the contrary, no colonies from the control group produced 15% higher Trp than the initial strain, whereas ~76% (73/96) strains showed similar and decreased Trp production in the control group. To further verify that the phenotype of the sorted strains was stable and reproducible, the top four colonies as well as strain KW003 were cultivated and fermented in 250 mL shake flasks. It was found that the fermentation results of these five strains in shake flasks were in a good agreement with those in 96-well microplates (Figure S3b). These results confirmed that FADS, combined with a biosensor, was a powerful tool to achieve the desired phenotypes with the advantages of a short period, convenient operation, and high efficiency.

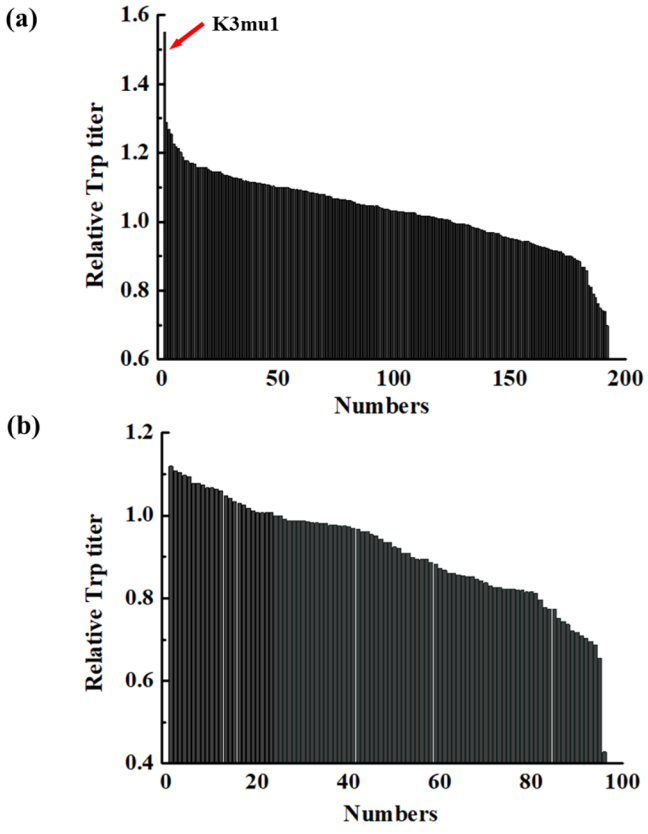

Figure 3. Trp production of strains screened by FADS or picked up randomly. The KW003 strain carrying p15-ribo727 was treated with the ARTP mutagenesis system to generate a random mutagenesis library. Mutants were cultivated on LB plates at 37 °C overnight. (a) Colonies that survived on the LB agar plates were collected and screened by FADS. The screened cells were cultivated in 96-well microtiter plates, and Trp titers were determine by an MAA assay. The top-performing strain was named K3mu1. (b) Mutants that survived on the LB agar plate were randomly selected as a control.

Genome Sequence of Mutant K3mu1. To get a better understanding of the hyperproduction mechanism of K3mu1, whole-genome sequencing was performed on this strain. A total of 11 942 244 reads were obtained, 94.8% of which were properly mapped into the reference genome. Genome alignment analysis revealed that 10 single-nucleotide polymorphism (SNPs) were manifested in the genome of K3mu1, among which 7 were nonsynonymous mutations, 1 was a synonymous mutation, and the other 2 were in the upstream or downstream of gene-coding sequences (Table S3). The nonsynonymous SNPs located in the genes involved in cell motility (*filL*), glucarate catabolism (*garL*), transporters (*yeeO*, *yhjV*), lipoate biosynthesis (*lplA*), and global transcriptional regulators (*crp*). As far as we know, none of these SNPs have been previously reported in Trp or other amino acid industrial strains.

To investigate the roles of nonsynonymous SNPs in K3mu1, a series of strains derived from K3mu1 were constructed by introducing an individual back-mutation into the chromosome via CRISPR-Cas9-mediated genome editing. All of the mutants were cultivated in parallel, and their growth conditions, Trp titers, and yields were measured. As a result, six mutants presented a similar growth condition as the K3mu1 strain, indicating that these SNPs had no influence on the physiological functions of K3mu1. One exception was K3m-crp^{wt}, whose final OD was lower than that of other strains (reaching 8.59) and similar to that of the KW003 strain (Figure 4a). In addition, K3m-crp^{wt} produced 1.41 g/L Trp with a yield of 0.102 g/g glucose (Figure 4b), which was 35.3% and 8.93% lower than that of K3mu1, respectively. In contrast, the other mutants did not show obvious differences in Trp yields or titers compared with K3mu1. These results clearly demonstrated that the SNP on *crp* played a significant role in the improvement of Trp production inK3mul.

Influence of CRP Mutant on Trp-Producing Strain. To further elucidate the function of CRP(T29K) in K3mu1, transcriptomes of K3mu1 and K3m-crp^{wt} were analyzed to observe the transcriptional changes between them. Transcriptome analysis demonstrated that CRP(T29K) resulted in simultaneous changes to the expression levels of multiple genes. Specifically, 646 genes (221 up-regulated and 425 down-regulated genes) displayed great expression level changes in K3mu1 by more than two-fold at a *P*-value threshold of < 0.05 (Figure 5a). Gene ontology enrichment analysis revealed that the up-regulated genes were mainly

https://doi.org/10.1021/acssynbio.0c00647
ACS Synth. Biol. 2021, 10, 1373−1383

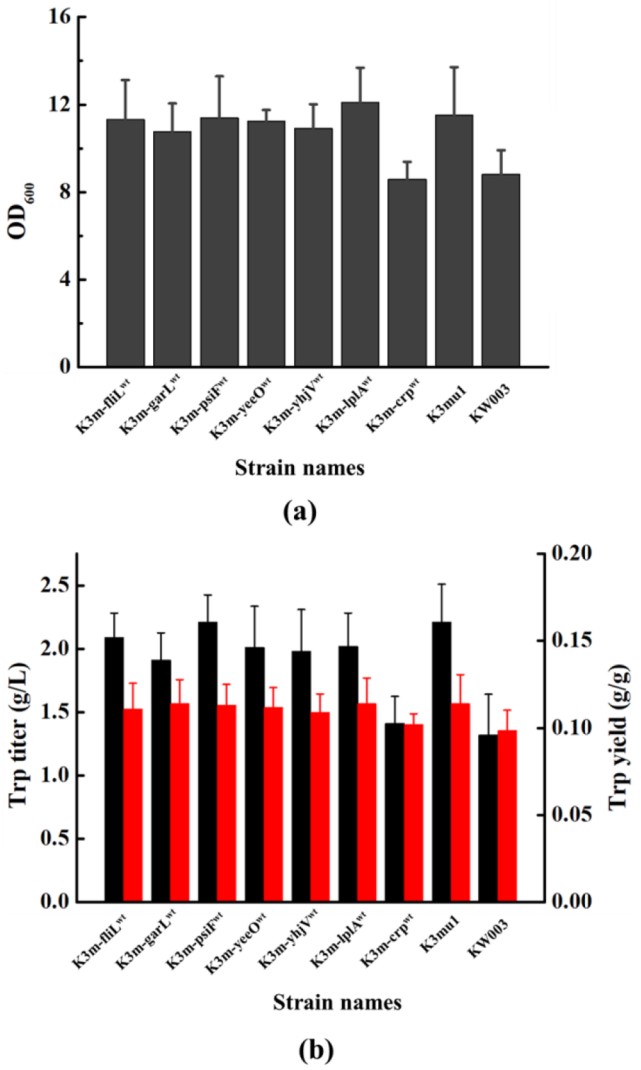

Figure 4. Fermentation results of K3mu1 and its derivative strains that were produced by back mutations. The KW003 strain was taken as a control and cultivated in parallel. After 42 h of fermentation, the OD, Trp titers, and Trp yields of all strains were measured. All of the fermentation experiments were carried out in triplicate.

associated with protein folding (*e.g., groS, grpE, hslO, dnaJ, htpG*), the macromolecule catabolic process (*e.g., clpS, yoeB, amiD, csrA, hslV*), the response to stress (*e.g., htpG, mutM, uspA, katG, mfd, sbcB*), and the oxidation−reduction process (*e.g., ldhA, dadA, nrdE, hmp, maeB*), whereas the down-regulated genes belonged to the peptide metabolic process (*e.g., rplY, rplK, rpsF, rpsT, rpsU*), translation (*e.g., efp, rplM, glyS, glyQ*), and the amide biosynthetic process (*e.g., rpmA, rpsM, rpsK, rpmJ, proS*) (Figure 5b). Among the genes that exhibited different expression levels, only 16 genes were directly up-regulated by CRP, whereas genes that were indirectly or not regulated by CRP constituted ∼96.2% of the up-regulated genes. The genes or operons that are repressed by CRP were not found in the down-regulated genes. This implied that CRP(T29K) not only altered the expression profiles of its regulated genes but also affected the genes that were not directly regulated by CRP. In addition, genes that altered transcriptional levels may also be regulated by other global transcript factors, indicating a complex regulation network.

Afterward, the focus was shifted to the enzymes involved in the synthesis of Trp from glucose. Compared with K3mu1-crp^{wt}, half of the enzymes in the glycolysis pathway were up-regulated more than two-fold, whereas enzymes in the pentose phosphate (PP) pathway showed a similar or lower level in K3mul (Figure 5c). Most notable was the tricarboxylic acid (TCA) cycle, in which enzymes from oxaloacetate (OAA) to α-ketogluturic acid (AKG) were up-regulated, whereas enzymes converting AKG to OAA were down-regulated in K3mul. As for the precursors to Trp synthesis, genes in 5-phospho-α-D-ribose 1-diphosphate (PRPP) and serine pathways showed no obvious difference between the two strains, but genes coding for glutamine synthesis were drastically down-regulated in K3mul. The majority of genes in the shikimate pathway and the Trp operon in K3mul were moderately up-regulated by less than two-fold. Overall, CRP(T29K) did not bring huge perturbations for PP pathways and Trp biosynthesis in K3mu1 but resulted in changes in the glycolysis pathway and the TCA cycle. AKG was a key node in the central pathway: Genes involved in its synthetic pathway were up-regulated, but genes associated with AKG degradation showed decreased expression levels. It is plausible that some genes coding stress-induced enzymes might be up-regulated in K3mu1, and these enzymes either required AKG as the cosubstrate or directed catalyzed AKG to generate some secondary metabolites that could facilitate K3mu1 to adapt to the harsh environment. This was in accordance with transcriptome results that showed that a large number of genes coding for the stress response were up-regulated in K3mu1.

To confirm this inference, the growth performances of KW003, K3mu1, and K3mu1-crp^{wt} were observed under various stressful conditions. All strains were cultivated in 250 mL shake flasks containing 50 mL of M9 medium supplemented with 0.4 M NaCl, 4 mM H_2O_2, or 10 mM acetate. In addition, growth conditions of these three strains in M9 medium were observed as well. As shown in Figure 6a, the growth curves of KW003, K3mu1, and K3mu1-crp^{wt} were similar in M9 medium. When 0.4 M NaCl was added to the medium, the growth of all strains was strongly hindered. The OD of K3mu1 reached 0.11 after 8 h and kept growing after 16 h. On the contrary, the growth of KW003 and K3mu1-crp^{wt} was completely stopped in the presence of 0.4 M NaCl (Figure 6b). Similarly, the growth of KW003, K3mu1, and K3mu1-crp^{wt} was inhibited in the M9 medium containing 10 mM acetate (Figure 6c), but K3mu1 exhibited a better growth performance than KW003 and K3mu1-crp^{wt}. The final OD of K3mu1 was ∼0.26, 1.94 and 2.07 times higher than that of K3mu1-crp^{wt} and KW003. Moreover, these three strains presented poor growth when 4 mM H_2O_2 was added to the M9 medium. The OD of three strains peaked at 10 h and began to drop after that, but the decreased rate of K3mu1 was lower than that of K3mu1-crp^{wt} and KW003 (Figure 6d). Taken together, these results indicated that K3mul had more excellent resistance toward various harsh environments than K3mu1-crp^{wt} and KW003. Interestingly, the growth curves of K3mu1-crp^{wt} and KW003 were almost similar under different stressful environments, indicating that except for CRP(T29K), the other nine SNPs found in the genome of K3mu1-crp^{wt} had no significant effect on its growth.

To further its function in the *E. coli* wild-type strain, we introduced CRP(T29K) into the *E. coli* W3110 strain to yield the W3110-crp strain. Both W3110 and W3110-crp were

https://doi.org/10.1021/acssynbio.0c00647
ACS Synth. Biol. 2021, 10, 1373−1383

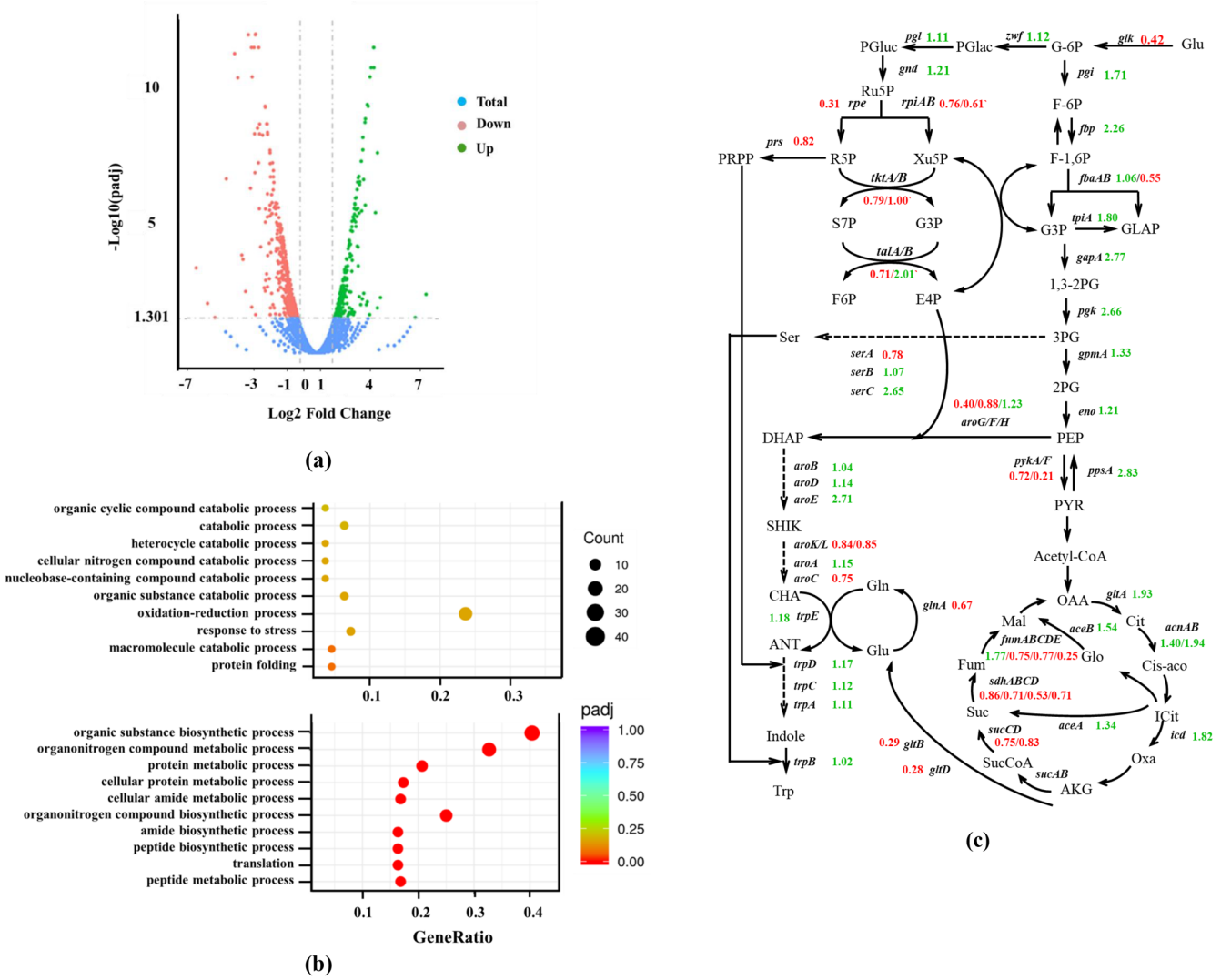

Figure 5. Transcriptome analysis of K3mu1 and K3m-crp^{wt}. (a) Volcano map of genes that show different expression levels in K3mu1 and K3m-crp^{wt}. (b) GO function enrichment bubble plot of genes that show different expression levels in K3mu1 and K3m-crp^{wt}. "GeneRatio" represents the ratio of the number of differential genes annotated to the GO to the total number of differential genes. "padj" is the *P* value after multiple hypothesis testing. "Count" is the number of differential genes annotated to the GO. (c) Differential expression levels of genes involved in Trp synthesis in K3mu1 and K3m-crp^{wt}. Glu, glucose; G-6P, glucose-6-phosphate; F-6P, fructose-6-phosphate; F-1,6P, fructose-1,6-bisphosphate; G3P, glyceraldehyde-3-phosphate; 3PG, glycerate-3-phosphate; 2PG, glycerate-2-phosphate; PEP, phosphoenolpyruvate; PYR, pyruvate; acetyl-CoA, acetyl coenzyme A; OAA, oxalosuccinate; Cit, citric acid; Cis-aco, cis-aconitase; ICit, isocitrate; Oxa, oxalosuccinate; AKG, α-ketoglutarate; SucCoA, succinyl-CoA; Suc, succinate; Fum, fumarate; Mal, malate; PGluc, 6-phosphate-glucose lactone; Ru5P, ribulose-5-phosphate; Xu5P, xylulose-5-phosphate; R5P, ribose-5-phosphate; S7P, sedoheptulose-7-phosphate; E4P, erythrose-4-phosphate; PRPP, 5-phospho-α-D-ribose 1-diphosphate; Ser, L-serine; DAHP, 3-deoxy-D-arabinoheptulosonate 7-phosphate; SHIK, shikimate; CHA, chorismate; ANT, anthranilate.

cultivated in shake flasks in parallel, and their growth conditions were determined under the same stressful conditions as those described in Figure 6. Unfortunately, both strains could not survive under such harsh conditions (Figure S4a). This can be interpreted by the fact that KW003 was derived from *E. coli* W3110 through multiple rounds of random mutagenesis and screening, which resulted in its strong resistance to different stresses. To this end, we reduced the concentrations of NaCl, acetate, and H_2O_2, under which conditions strains W3110 and W3110-crp suffered growth arrest but still survived. The final concentrations of NaCl, acetate, and H_2O_2 were determined to be 50, 0.1, and 0.1 mM, respectively. As can be seen in Figure S4b, the growth of both W3110 and W3110-crp was inhibited to a different extent when 50 mM NaCl, 0.1 mM acetate, or 0.1 mM H_2O_2 was added to the M9 medium. However, no significant differences were observed when compared with the growth of W3110 and W3110-crp under various stressful environments, indicating that CRP(T29K) had no obvious effect on the improvement in resistance for the W3110 strain. We speculated that some other SNPs on the chromosome of KW003,[25] together with CRP(T29K), may improve the cell's resistance in a combined manner.

In this study, an HTS platform for Trp-producing strains was constructed by coupling a riboswitch-based Trp biosensor and FADS technology, which highlighted the potential application of biosensors to monitoring and detecting inconspicuous compounds. Novel aptamers can be obtained through SELEX or structure-based rational design. However, most aptamers achieved are found to be feedback-inhibited by

https://doi.org/10.1021/acssynbio.0c00647
ACS Synth. Biol. 2021, 10, 1373−1383

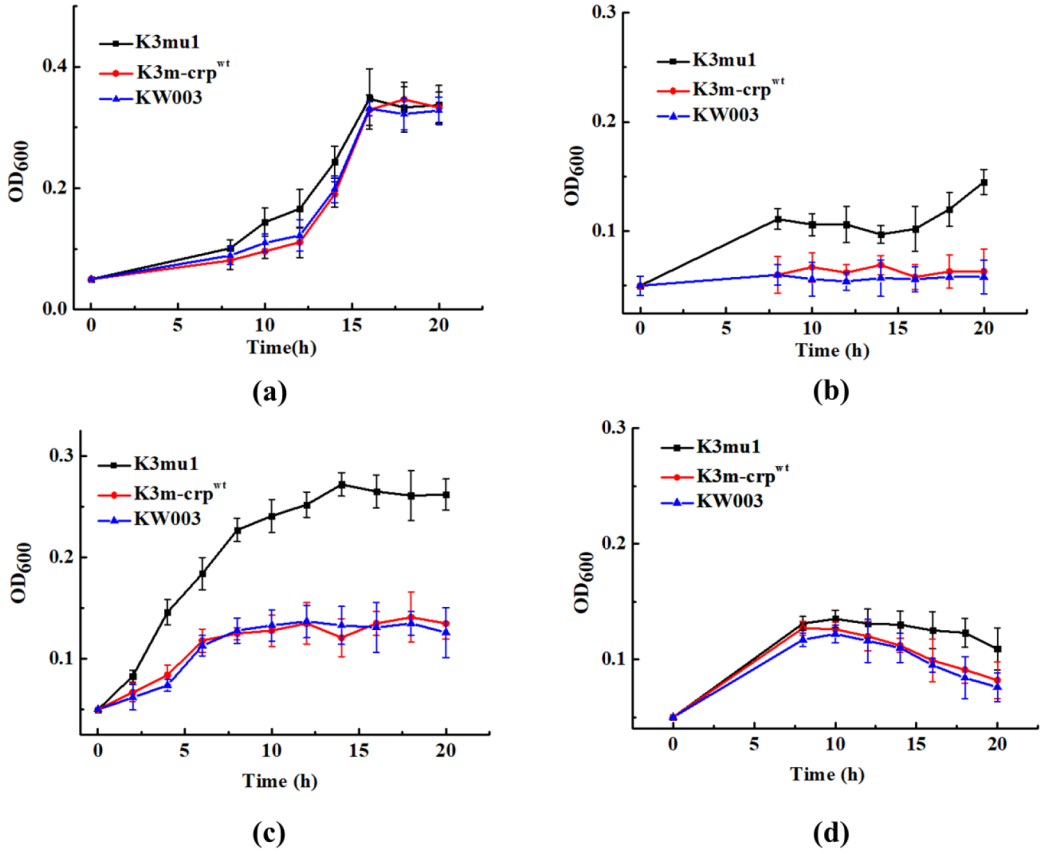

Figure 6. Growth curves of KW003, K3mu1, and K3m-crp^{wt} under various stressful conditions. Both strains were cultivated in the 250 mL shake flasks containing 50 mL of M9 medium (a) or supplemented with 0.4 M of NaCl (b), 10 mM of acetate (c), or 4 mM of H_2O_2 (d). All of the results were carried out in triplicate.

a ligand compound, which cannot be directly applied as a screening tool for the HTS of industrial strains. Fortunately, the two Trp aptamers we employed showed a positive correlation with Trp concentrations. These two aptamers had different structures: ribo-727 contained a CYA motif (5′-CGCYACY-3′), whereas ribo-585 did not.[24] Ribo585 behaved like a typical "natural riboswitch": It transformed from the "OFF" state to the "ON" state when the concentration of the inducer reached a certain level. On the contrary, ribo727 activated the expression level of the downstream gene in a gradient-like manner. Because of this, ribo727 was more suitable to construct Trp biosensor from the industrial application point of view. In fact, bases that protected against DMS (dimethyl sulfate) or CMCT (1-cyclohexyl-3-[morpholynoethyl) modification by Trp binding were both discovered on ribo585 and ribo727. However, ribo727 contained bases that are more accessible to modification by Trp binding and bases that interfere with binding to Trp, which were not found in ribo585.[24] It is speculated that these bases in ribo727 prevent its drastic conformation change in response to the elevated Trp concentrations.

Microfluidics provides useful tools that play significant roles in advanced biochemical research and development. One of its significant applications in the field of synthetic biology is that the HTS platform based on droplet-based microfluidic technology allows the rapid evolution of industrial strains for the hyperproduction of desired compounds. The screening ability is further strengthened by the fact that the droplet allows a close imitation of controlled cultivation conditions so that the reliability of such a screening process is improved. Compared with agar-plate screening and FACS technology, droplet microfluidic technology has several advantages. First, agar-plate screening often contains high concentrations of antibiotic that is used to kill the mutants with poor production capabilities. However, a high dosage of antibiotic may also cause physiological injury to cells. In addition, mutations that develop a resistance to the antibiotic can better survive on agar plates, which increases the possibility of false-positive strains. FADS, however, does not require the addition of an antibiotic, so the negative effects of the antibiotic will be avoided. Second, the interpretation of FACS results may be complicated because of the overlapping fluorescence profiles and the anomalous fluorescence due to the cell's heterogeneity. On the contrary, FADS promises that the majority of cells are individually encapsulated in microdroplets, and the subsequent proliferation and production are also carried out in microdroplets. In this way, interactions between cells (such as quorum sensing) are cut off so that the anomalous fluorescence can be kept to a minimum. Third, unlike FACS, which is dependent on a single cell's fluorescence value, FADS is based on the sum of all strains' fluorescence values in the droplet. In other words, FADS only selects the mutants that produce a high amount of product during the cultivation process.

CRP is a crucial transcript factor that regulates 192 genes or regulons and harmonizes several genetic circuits at the transcriptional level,[26] which makes it a potential target for global transcription machinery engineering (gTME). For instance, CRP has been successfully engineered via directed

https://doi.org/10.1021/acssynbio.0c00647
ACS Synth. Biol. 2021, 10, 1373−1383

Table 1. Strains and Plasmids Used in This Study

strains/plasmid	description	source
Plasmids		
p15A		Fang[38]
p15-ribo585	P15A vector carrying aptamer ribo585	this work
p15-ribo727	P15A vector carrying aptamer ribo727	this work
pRedCas9	applied for genome editing	Zhao[33]
pCas-tesB	derivative from pRedCas9 plasmid, applied for construction of K3m-tesB^{wt}	this work
pCas-fliL	applied for construction of K3m-fliL^{wt}	this work
pCas-garL	applied for construction of K3m-garL^{wt}	this work
pCas-psiF	applied for construction of K3m-psiF^{wt}	this work
pCas-yeeO	applied for construction of K3m-yeeO^{wt}	this work
pCas-yhjV	applied for construction of K3m-yhjV^{wt}	this work
pCas-lplA	applied for construction of K3m-lplA^{wt}	this work
pCas-crp	applied for construction of K3m-crp^{wt}	this work
Strains		
KW	derived from *E. coli* W3110, engineered for Trp production	Chen[25]
KW001	derived from KW strain	Chen[25]
KW002	derived from KW strain	Chen[25]
KW003	derived from KW strain	Chen[25]
K3mu1	derived from KW003, obtained by FADS	this work
K3mu2	derived from KW003, obtained by FADS	this work
K3mu3	derived from KW003, obtained by FADS	this work
K3mu4	derived from KW003, obtained by FADS	this work
K3m-fliL^{wt}	derived from K3mu1, produced by back mutation of *fliL* (T61I)	this work
K3m-garL^{wt}	derived from K3mu1, produced by back mutation of *garL* (A190S)	this work
K3m-psiF^{wt}	derived from K3mu1, produced by back mutation of *psiF* (A49V)	this work
K3m-yeeO^{wt}	derived from K3mu1, produced by back mutation of *yeeO* (G272E)	this work
K3m-yhjV^{wt}	derived from K3mu1, produced by back mutation of *yhjV* (G155D)	this work
K3m-lplA^{wt}	derived from K3mu1, produced by back mutation of *lplA* (G137D)	this work
K3m-crp^{wt}	derived from K3mu1, produced by back mutation of *crp* (T29K)	this work

evolution to improve the strain's performance under various stressful environment, such as osmotolerance,[27] oxidative stress,[28] and organic solvent tolerance[29] which are often encountered during bioprocessing. In these cases, the introduction of one or two mutations in CRP often results in obvious phenotypic alteration. Strain phenotypes are determined by the translation products of thousands of genes and the multiple layers of interconnected regulation networks that govern them. The modification of transcription factors may result in a perturbation of the transcriptome of the strain by changing the DNA binding specificity, the interaction between transcription factors, or the chaperone proteins.[30] Thus the cellular transcriptional profile may be completely altered by simple modifications of CRP.[31] CRP is composed of a cAMP binding N-terminal domain (NTD), a DNA binding C-terminal domain (CTD), and a hinge region that connects NTD and CTD. Previous work showed that mutation sites that enabled strains to acquire elevated tolerance under stressful environment were distributed in all three regions. Most of these sites were located in the cAMP binding pocket (G71D/C, R82C, V86L), C-helix region (M114V, Q119N, K130E), and D-helix region (V139M, T146I).[27−29,32] These mutations played a crucial role in allosteric signal generation and transmission, maintaining the interaction between NTD and CTD or the intersubunit communication of CRP. So far, CRP(T29K) has not been reported to improve the production of aromatic amino acids in *E. coli*. In this contribution, it is confirmed that the introduction CRP(T29K) into a Trp-producing strain successfully improved its resistance toward high osmotolerance, low pH, and oxidative stress. Because this mutation site is close to the cAMP binding pocket, one possible explanation is that CRP(T29K) affects the interaction between CRP and cAMP and consequently enhances its activation effects on the genes involved in antistress genes. Thus K3mu1 remained robust even in the stationary phase of the fermentation and finally improved the Trp production.

MATERIALS AND METHODS

Bacterial Strains, Plasmids, and Cultivation Medium. All of the strains and plasmids used in this study are listed in Table 1. DNA fragments "ribo-585" and "ribo-727" were synthesized by GENEWIZ Company (China). *Escherichia coli* (*E. coli*) DH5α (Transgene, Beijing) was used for plasmid construction. Primers that were used in this study are shown in Table S1. pRedCas9 was a kind gift from D. Zhao and was used for genome editing in *E. coli*.[33]

For 96-well plate fermentation, individual colonies were cultivated in 96-deep-well assay blocks (Corning Costar 3960, square V-bottom, 2 mL) containing 500 μL of Luria broth (LB) medium per well overnight. Strains were subsequently inoculated in 500 μL of fermentation medium (30 g/L glucose, 0.5 g/L $MgSO_4{\cdot}7H_2O$, 3 g/L KH_2PO_4, 12 g/L K_2HPO_4, 4 g/L $(NH_4)_2SO_4$, 1 g/L yeast extract, 2 g/L monosodium citrate, and 0.1 g/L $FeSO_4{\cdot}7H_2O$) at 37 °C, 900 rpm, 80% humidity for 42 h in a Microtron shaker (Infors, China).

For shake flask fermentation, a single colony selected from the agar plate was inoculated in 5 mL of LB medium overnight and then inoculated in a 250 mL flask containing 20 mL of fermentation medium and afterward cultivated at 37 °C, 200 rpm for 42 h.

https://doi.org/10.1021/acssynbio.0c00647
ACS Synth. Biol. 2021, 10, 1373−1383

Construction of the Random Mutagenesis Library Using ARTP. A single colony of KW003 strain carrying p15-ribo727 was picked from the agar plate and cultivated in LB medium overnight. The next day, cells were inoculated in fresh LB medium with an inoculation ratio of 1:250. When the strain's OD_{600} reached 1.0, cells were collected and washed by phosphate-buffered saline (PBS) buffer (8.0 g/L NaCl, 0.2 g/L KCl, 1.44 g/L Na_2HPO_4, 0.24 g/L KH_2PO_4) three times and resuspended by PBS buffer. The suspension was treated with an ARTP biological mutagenesis system (ARTP-II, Beijing) according to the manufacturer's instruction. The mutation time was tested from 10 to 20 s at intervals of 1 s. The optimized mutation time was determined with the criterion that the mortality of cells was ∼90%. After mutagenesis, living cells were then collected in PBS buffer for subsequent screening.

Screening of Mutant Strains with Increased Trp Production. Cells that were treated by ARTP were diluted by mixing in LB medium to a final OD_{600} of 0.1. Droplets were generated in a microfluidic flow-focusing device using this culture as the aqueous phase and fluorinated oil with a surfactant as the oil phase. The flow rates were 100 and 300 μL/h for the aqueous and oil phases, respectively. 6 pL droplets were generated at a rate of 3000/s to maintain the cell-to-droplet ratio at 0.3. Droplets were then collected into 1 mL syringes (BD Biosciences, USA) and incubated at 30 °C for 4 h. After incubation, the droplets were reinjected into the microfluidic sorting device. The sorting process was performed with a flow rate of 10 μL/h droplets and 200 μL/h fluorinated oils to space the droplets. In the sorting device, the droplets were excited with a 473 nm laser, and the fluorescence signal of each droplet was detected by the droplet microfluidic system. Droplets with fluorescence intensity that exceeded the predefined threshold were sorted by dielectrophoresis. The sorted droplets were collected in a 1.5 mL tube. After sorting was completed, cells were recovered from the sorted droplets and seeded on agar plates.

Determination of Trp Titers of Strains Cultivated in a 96-Well Plate. In the acidic environment (pH 2.75), MAA reacts with Trp, and the product can be detected at an excitation of 253 nm and an emission of 450 nm. The fluorescence intensity is linear in the range of 0−100 mg/L Trp. On the basis of this information, a 96-well-plate-based determination of the Trp amount assay was developed as follows: 10 μL of samples was added to 200 μL of reaction buffer (0.3% MAA, 0.4 mM $NaNO_2$, 0.1 M citrate, 0.2 M $Na_2HPO_4{\cdot}12H_2O$, pH 2.75). After incubation at 80 °C for 10 min, the fluorescence values of the reaction systems were measured by a microplate reader system (HITACHI).

Determination of Intercellular Trp Concentration. The extraction of cytoplasm intermediates was carried out according to a previous report.[34] To prepare the cell extract, 500 μL of cell suspension was precipitated by centrifugation in a 1.5 mL tube containing 100 μL of silicone oil. After centrifugation, the supernatant was removed, and cell pellets were resuspended by adding 200 μL of perchloric acid (20% v/v) under gentle mixing. After disruption by sonication, 200 μL of Na_2CO_3 was added to the tube to neutralize the solution. The supernatant was then filtered and stored at −20 °C for subsequent high-performance liquid chromatography (HPLC) analysis. For *E. coli*, the ratio of cell volume to cellular dry weight is 0.0023 L/g,[35] and the correlation relating to the dry cell weight to OD_{600} for *E. coli* W3110 was determined to be 0.346 g/L/OD_{600}.[36]

Genomic Editing by CRISPR-Cas9 System. The construction of back mutants of K3mu1 was carried out by the CRISPR-Cas9 system. To construct gene-specific double-strand donor DNA (dsDNA), two mutation sites were simultaneously introduced into dsDNA. One was the target mutation and the other one was a synonymous mutation in the "NGG" PAM sequence so that colonies edited by CRISPR-Cas9 system survived on the agar plate containing 0.2% arabinose. The dsDNA was then ligated into pRedCas9 and transformed into the electrocompetent cells. The electroporation parameters were as follows: 0.1 cm cuvette, 1.70 kV (Bio-Rad MicroPulser). After cells were cultivated on LB agar plate containing 0.2% arabinose, strains that survived on the plate were verified by polymerase chain reaction (PCR) and DNA sequencing.

RNA Extraction and Transcriptome Analysis. Cells were grown at 37 °C overnight in 5 mL of LB medium supplemented with 15 μg/mL tetracycline. The following day, cells were inoculated in 50 mL of fermentation medium with an inoculation ratio of 1:25 and continued to cultivate for 17.5 h. Cells were harvested in the early stationary phase by centrifugation at 4000 *g* for 15 min at 4 °C and then treated with liquid nitrogen for RNA isolation. The TRIzol RNA extraction kit (BioTNT, China) was used to extract the RNA. The quality of RNA (including RNA quantity and RNA degradation) was monitored by an Agilent 2100 bioanalyzer (Agilent, USA). Then, ribosome RNA (rRNA) was removed from the total RNA, and the messenger RNA (mRNA) was randomly broken into small fragments for the subsequent sequencing.[37]

■ ASSOCIATED CONTENT

Supporting Information

The Supporting Information is available free of charge at https://pubs.acs.org/doi/10.1021/acssynbio.0c00647.

Table S1. Primers used in this study. Table S2. Sequences of ribo-585 and ribo-727. Table S3. List of SNPs in the K3mu1 strain. Figure S1. YFP values of *E. coli* carrying p15-ribo727 in response to 20 kinds of canonical amino acids. Figure S2. Lethality curve of strains treated with different mutation times. Figure S3. Fermentation results for KW003 and its derivative strains produced by back mutation in shake flasks. Figure S4. Growth conditions of *E. coli* W3110 and W3110-crp under various stressful environments. (PDF)

■ AUTHOR INFORMATION

Corresponding Author

Dawei Zhang − *Tianjin Institute of Industrial Biotechnology, Chinese Academy of Sciences, Tianjin 300308, China; Key Laboratory of Systems Microbial Biotechnology, Chinese Academy of Sciences, Tianjin 300308, China; National Engineering Laboratory for Industrial Enzymes, Tianjin 300308, China;* orcid.org/0000-0002-5857-394X; Email: zhang_dw@tib.cas.cn

Authors

Yongfei Liu − *Tianjin Institute of Industrial Biotechnology, Chinese Academy of Sciences, Tianjin 300308, China; Key Laboratory of Systems Microbial Biotechnology, Chinese*

https://doi.org/10.1021/acssynbio.0c00647
ACS Synth. Biol. 2021, 10, 1373−1383

Academy of Sciences, Tianjin 300308, China; National Engineering Laboratory for Industrial Enzymes, Tianjin 300308, China

Huiling Yuan − *Tianjin Institute of Industrial Biotechnology, Chinese Academy of Sciences, Tianjin 300308, China; Key Laboratory of Systems Microbial Biotechnology, Chinese Academy of Sciences, Tianjin 300308, China; National Engineering Laboratory for Industrial Enzymes, Tianjin 300308, China*

Dongqin Ding − *Tianjin Institute of Industrial Biotechnology, Chinese Academy of Sciences, Tianjin 300308, China; Key Laboratory of Systems Microbial Biotechnology, Chinese Academy of Sciences, Tianjin 300308, China; National Engineering Laboratory for Industrial Enzymes, Tianjin 300308, China*

Huina Dong − *Tianjin Institute of Industrial Biotechnology, Chinese Academy of Sciences, Tianjin 300308, China; Key Laboratory of Systems Microbial Biotechnology, Chinese Academy of Sciences, Tianjin 300308, China; National Engineering Laboratory for Industrial Enzymes, Tianjin 300308, China*

Qinhong Wang − *Tianjin Institute of Industrial Biotechnology, Chinese Academy of Sciences, Tianjin 300308, China; Key Laboratory of Systems Microbial Biotechnology, Chinese Academy of Sciences, Tianjin 300308, China; National Engineering Laboratory for Industrial Enzymes, Tianjin 300308, China;* orcid.org/0000-0003-0004-2721

Complete contact information is available at: https://pubs.acs.org/10.1021/acssynbio.0c00647

Author Contributions

Y.L., H.Y., and D.Z. designed the experiments and wrote the manuscript. Y.L., D.D., H.D., Q.W., and D.Z. performed the experiments and analyzed the data.

Notes

The authors declare no competing financial interest.

■ ACKNOWLEDGMENTS

This work was supported by the National Key R&D Program of China (2020YFA0907800), the National Natural Science Foundation of China (NSFC 31800086), and Tianjin Synthetic Biotechnology Innovation Capacity Improvement Project (TSBICIP-KJGG-004-03).

■ REFERENCES

(1) Zhang, M. M., Wang, Y., Ang, E. L., and Zhao, H. (2016) Engineering microbial hosts for production of bacterial natural products. *Nat. Prod. Rep. 33*, 963−987.

(2) Lee, S. Y., and Kim, H. U. (2015) Systems strategies for developing industrial microbial strains. *Nat. Biotechnol. 33*, 1061−1072.

(3) Raman, S., Rogers, J. K., Taylor, N. D., and Church, G. M. (2014) Evolution-guided optimization of biosynthetic pathways. *Proc. Natl. Acad. Sci. U. S. A. 111*, 17803−17808.

(4) Gasch, A. P., Spellman, P. T., Kao, C. M., Carmel-Harel, O., Eisen, M. B., Storz, G., Botstein, D., and Brown, P. O. (2000) Genomic expression programs in the response of yeast cells to environmental changes. *Mol. Biol. Cell 11*, 4241.

(5) Chang, A. L., Wolf, J. J., and Smolke, C. D. (2012) Synthetic RNA switches as a tool for temporal and spatial control over gene expression. *Curr. Opin. Biotechnol. 23*, 679−688.

(6) Liu, D., Evans, T., and Zhang, F. (2015) Applications and advances of metabolite biosensors for metabolic engineering. *Metab. Eng. 31*, 35−43.

(7) Wachsmuth, M., Findeiss, S., Weissheimer, N., Stadler, P. F., and Morl, M. (2013) De novo design of a synthetic riboswitch that regulates transcription termination. *Nucleic Acids Res. 41*, 2541−2551.

(8) Ramesh, A., and Winkler, W. C. (2010) Magnesium-sensing riboswitches in bacteria. *RNA Biol. 7*, 77−83.

(9) Baker, J. L., Sudarsan, N., Weinberg, Z., Roth, A., Stockbridge, R. B., and Breaker, R. R. (2012) Widespread genetic switches and toxicity resistance proteins for fluoride. *Science 335*, 233−235.

(10) Miranda-Rios, J., Navarro, M., and Soberon, M. (2001) A conserved RNA structure (thi box) is involved in regulation of thiamin biosynthetic gene expression in bacteria. *Proc. Natl. Acad. Sci. U. S. A. 98*, 9736−9741.

(11) Lu, C., Smith, A. M., Fuchs, R. T., Ding, F., Rajashankar, K., Henkin, T. M., and Ke, A. (2008) Crystal structures of the SAM-III/S(MK) riboswitch reveal the SAM-dependent translation inhibition mechanism. *Nat. Struct. Mol. Biol. 15*, 1076−1083.

(12) Nahvi, A., Sudarsan, N., Ebert, M. S, Zou, X., Brown, K. L, and Breaker, R. R (2002) Genetic control by a metabolite binding mRNA. *Chem. Biol. 9*, 1043.

(13) Tuerk, C, and Gold, L (1990) Systematic evolution of ligands by exponential enrichment RNA ligands to bacteriophage T4 DNA polymerase. *Science 249*, 505.

(14) Ellington, A. D., and Szostak, J. W. (1990) In *vitro* selection of RNA molecules that bind specific ligands. *Nature 346*, 818.

(15) Findeiss, S., Etzel, M., Will, S., Morl, M., and Stadler, P. F. (2017) Design of Artificial Riboswitches as Biosensors. *Sensors 17*, 1990.

(16) Groher, F., Bofill-Bosch, C., Schneider, C., Braun, J., Jager, S., Geissler, K., Hamacher, K., and Suess, B. (2018) Riboswitching with ciprofloxacin-development and characterization of a novel RNA regulator. *Nucleic Acids Res. 46*, 2121−2132.

(17) Boussebayle, A., Torka, D., Ollivaud, S., Braun, J., Bofill-Bosch, C., Dombrowski, M., Groher, F., Hamacher, K., and Suess, B. (2019) Next-level riboswitch development-implementation of Capture-SELEX facilitates identification of a new synthetic riboswitch. *Nucleic Acids Res. 47*, 4883−4895.

(18) Zhou, L. B., and Zeng, A. P. (2015) Engineering a lysine-ON riboswitch for metabolic control of lysine production in *Corynebacterium glutamicum*. *ACS Synth. Biol. 4*, 1335−1340.

(19) Pham, H. L., Wong, A., Chua, N., Teo, W. S., Yew, W. S., and Chang, M. W. (2017) Engineering a riboswitch-based genetic platform for the self-directed evolution of acid-tolerant phenotypes. *Nat. Commun. 8*, 411.

(20) Fang, M., Wang, T., Zhang, C., Bai, J., Zheng, X., Zhao, X., Lou, C., and Xing, X. H. (2016) Intermediate-sensor assisted push-pull strategy and its application in heterologous deoxyviolacein production in *Escherichia coli*. *Metab. Eng. 33*, 41−51.

(21) Liu, Y., Zhuang, Y., Ding, D., Xu, Y., Sun, J., and Zhang, D. (2017) Biosensor-Based Evolution and Elucidation of a Biosynthetic Pathway in *Escherichia coli*. *ACS Synth. Biol. 6*, 837−848.

(22) Mazutis, L., Gilbert, J., Ung, W. L., Weitz, D. A., Griffiths, A. D., and Heyman, J. A. (2013) Single-cell analysis and sorting using droplet-based microfluidics. *Nat. Protoc. 8*, 870−891.

(23) Qiao, Y., Zhao, X., Zhu, J., Tu, R., Dong, L., Wang, L., Dong, Z., Wang, Q., and Du, W. (2018) Fluorescence-activated droplet sorting of lipolytic microorganisms using a compact optical system. *Lab Chip 18*, 190−196.

(24) Majerfeld, I., and Yarus, M. (2005) A diminutive and specific RNA binding site for L-tryptophan. *Nucleic Acids Res. 33*, 5482−5493.

(25) Chen, Y., Liu, Y., Ding, D., Cong, L., and Zhang, D. (2018) Rational design and analysis of an *Escherichia coli* strain for high-efficiency tryptophan production. *J. Ind. Microbiol. Biotechnol. 45*, 357.

(26) Zheng, D., Constantinidou, C., Hobman, J. L., and Minchin, S. D. (2004) Identification of the CRP regulon using *in vitro* and *in vivo* transcriptional profiling. *Nucleic acids research 32*, 5874−5893.

(27) Zhang, H., Chong, H., Ching, C. B., and Jiang, R. (2012) Random mutagenesis of global transcription factor cAMP receptor protein for improved osmotolerance. *Biotechnol. Bioeng. 109*, 1165−1172.
(28) Basak, S., and Jiang, R. (2012) Enhancing *E. coli* tolerance towards oxidative stress via engineering its global regulator cAMP receptor protein (CRP). *PLoS One 7*, No. e51179.
(29) Zhang, H., Chong, H., Ching, C. B., Song, H., and Jiang, R. (2012) Engineering global transcription factor cyclic AMP receptor protein of *Escherichia coli* for improved 1-butanol tolerance. *Appl. Microbiol. Biotechnol. 94*, 1107−1117.
(30) Tuch, B. B., Li, H., and Johnson, A. D. (2008) Evolution of Eukaryotic Transcription Circuits. *Science 319*, 1797.
(31) Atsumi, S., Wu, T. Y., Eckl, E. M., Hawkins, S. D., Buelter, T., and Liao, J. C. (2010) Engineering the isobutanol biosynthetic pathway in *Escherichia coli* by comparison of three aldehyde reductase/alcohol dehydrogenase genes. *Appl. Microbiol. Biotechnol. 85*, 651−657.
(32) Geng, H., and Jiang, R. (2015) cAMP receptor protein (CRP)-mediated resistance/tolerance in bacteria: mechanism and utilization in biotechnology. *Appl. Microbiol. Biotechnol. 99*, 4533−4543.
(33) Zhao, D., Yuan, S., Xiong, B., Sun, H., Ye, L., Li, J., Zhang, X., and Bi, C. (2016) Development of a fast and easy method for *Escherichia coli* genome editing with CRISPR/Cas9. *Microb. Cell Fact. 15*, 205.
(34) Trotschel, C., Deutenberg, D., Bathe, B., Burkovski, A., and Kramer, R. (2005) Characterization of methionine export in *Corynebacterium glutamicum*. *J. Bacteriol. 187*, 3786−3794.
(35) Bennett, B. D., Yuan, J., Kimball, E. H., and Rabinowitz, J. D. (2008) Absolute quantitation of intracellular metabolite concentrations by an isotope ratio-based approach. *Nat. Protoc. 3*, 1299−1311.
(36) Chen, L., and Zeng, A. P. (2017) Rational design and metabolic analysis of *Escherichia coli* for effective production of L-tryptophan at high concentration. *Appl. Microbiol. Biotechnol. 101*, 559−568.
(37) Parkhomchuk, D., Borodina, T., Amstislavskiy, V., Banaru, M., Hallen, L., Krobitsch, S., Lehrach, H., and Soldatov, A. (2009) Transcriptome analysis by strand-specific sequencing of complementary DNA. *Nucleic Acids Res. 37*, e123.
(38) Fang, H., Li, D., Kang, J., Jiang, P., Sun, J., and Zhang, D. (2018) Metabolic engineering of *Escherichia coli* for de novo biosynthesis of vitamin B12. *Nat. Commun. 9*, 4917.

https://doi.org/10.1021/acssynbio.0c00647
ACS Synth. Biol. 2021, 10, 1373−1383